Cosmic Ray Produced Antiprotons Confined in the Innermost Magnetosphere

H. Miyasaka,[1] A. Gusev,[2] G. Pugacheva,[3] N.J. Schuch,[3] U.B Jayanthi,[2] and W. Spjeldvik[4]

(1) RIKEN (The Institute of Physical and chemical Research), Japan
(2) National Institute for Space Research, Sao Jose dos Campos, Brazil
(3) Southern Regional Space Research Center/INPE, Santa Maria, Brazil
(4) Weber State University, Ogden, Utah, USA

Abstract

The possible existence of noticeable fluxes of antiparticles in the Earth magnetosphere is predicted on theoretical considerations here. We present the computational results of 50 MeV to several GeV antiproton fluxes produced from the CR particle interactions with the matter in the interstellar space and the residual atmosphere at altitudes of ∼1000 km over the Earth's surface. The estimates shows the magnetospheric antiproton fluxes are greater by two orders of magnitude compared to the interstellar fluxes measured at energies >1 GeV.

1. Introduction

Measurements of the interstellar antiproton spectrum generally support the idea of their secondary origin, i.e. they are produced in nuclear reactions with the interstellar matter by the primary cosmic rays (CR) in their chaotic motion in the galactic magnetic field during their lifetime in Galaxy. The same nuclear reactions of CR protons also happen in the Earth's atmosphere, including the uppermost residual atmosphere corresponding to high altitudes. In these nuclear reactions, a great variety of secondary particles are produced, including the secondary antiprotons. Part of the secondary particles born in the confinement region of the magnetosphere will be trapped in the Earth's geomagnetic field and create an antiproton radiation belt around the Earth. This belt is a product of the nuclear reactions similar to those of positron and isotope radiation belts [4, 7] created at the altitudes of about ∼1000 km above the Earth.

2. Antiproton production spectrum

For the modeling of the secondary nuclear reaction products, their spectra and the angular distributions, the nuclear reaction computer code SHIELD [3] was used. The simulations were performed to obtain spectra of the secondary
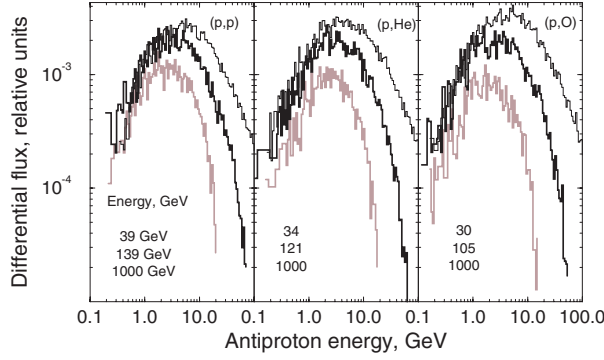
Fig. 1. The differential antiproton production spectra generated by protons with energy E_p on H, He and O target atomic nucleus.
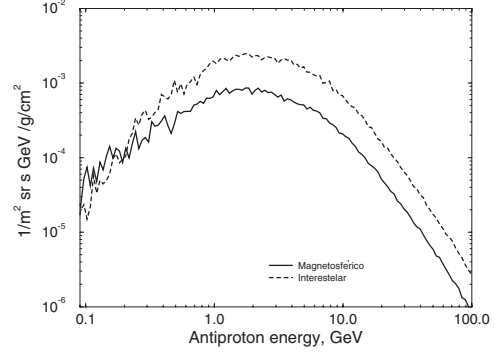
Fig. 2. The computed antiproton production spectra.

antiprotons and antineutrons The results of the simulation are shown in Fig 1.

Figures give examples of the differential secondary antiproton production spectra generated in 4π solid angle, $q(E_{\tilde{p}}, E_p)$, by one proton with energy E_p on one H, He and/or O target nucleus. The energy distributions at $E_p \sim 30$ GeV exhibit the characteristic flat maximum between antiproton energies of 1 - 2 GeV as observed in the various experiments [2 and references therein]. The antiproton production spectrum $(Q_{\tilde{p}}(E_{\tilde{p}}))$ from the CR proton spectrum (dN/dE_p) is obtained by numerical integration of the antiproton production spectrum $(q(E_{\tilde{p}}, E_p))$ over the CR spectra:

$$Q_{\tilde{p}}(E_{\tilde{p}}) = \xi \int\limits_{E_p,th}^{\infty} q(E_{\tilde{p}}, E_p) \frac{dN}{dE_p} dE_p \qquad (1)$$

Here ξ is a heavy nuclei correction factor of 1.25 describing the antiproton input which includes of the CR helium contribution [6]. The CR proton spectrum from the balloon experiment CAPRICE [1] was utilized:

$$\frac{dN}{dE_p} = (1.1 \pm 0.11) \cdot 10^{-4} E_p^{-2.73 \pm 0.06} \ (m^2 \cdot sr \cdot s \cdot GeV)^{-1} \ for \ E_p > 20 GeV \quad (2)$$

The authors demodulated the measured spectrum for the solar activity and obtained the interstellar spectrum:

$$\frac{dN}{dR} = (2.72 \pm 0.02) \cdot 10^4 E_p^{-2.928 \pm 0.004} \ (m^2 \cdot sr \cdot s \cdot GeV)^{-1} \ for \ R = 1.7 - 200 GV \quad (3)$$

3. Interstellar antiproton flux

In the computations of the antiproton production spectra through Eq.1 we utilized the interstellar proton spectrum (Eq.3) and the CR proton spectrum
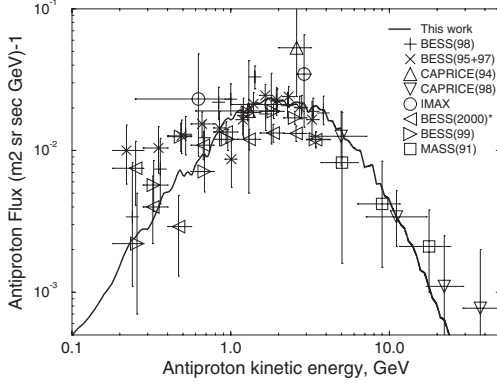
Fig. 3. The comparison of the computed and measured galactic antiproton flux.
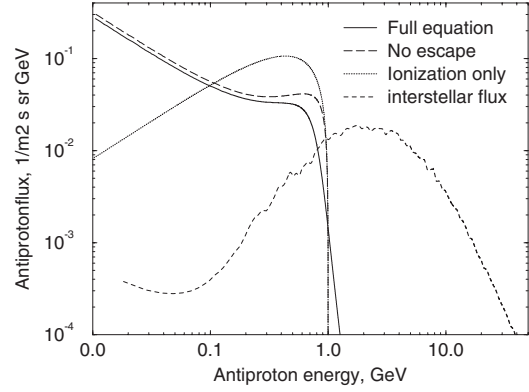

Fig. 4. The magnetospheric antiproton flux at L=1.2.

modulated by solar activity (Eq.2) to obtain the interstellar and the atmospheric antiproton production spectra respectively. Multiplying the integral (Eq.1) by factor $\sigma_{inel}N_A/A$ that takes into account the elemental composition of interstellar space and of the atmosphere, the antiproton production spectra per g/cm^2 of the matter are obtained separately (Fig 2.). The interstellar antiproton flux is defined by a continuity equation related to the leaky-box model:

$$F_{\tilde{p}}(E_{\tilde{p}})/\lambda_{esc} + F_{\tilde{p}}(E_{\tilde{p}})/\lambda_{inel} + \frac{d}{dE_{\tilde{p}}}\left(F_{\tilde{p}}(E_{\tilde{p}}) \cdot \frac{dE_{\tilde{p}}}{dX}\right) = Q_{\tilde{p}}(E_{\tilde{p}}) \qquad (4)$$

Here λ_{esc}, $\lambda_{inel} = \sigma_{inel}N_A/A$ are the escape [5] and the interaction length of antiprotons in the Galaxy. The third term defines the antiproton ionization energy losses and $(Q_{\tilde{p}}(E_{\tilde{p}}))$ is antiproton production spectrum. The Eq.4 was numerically solved by Runge-Kutta method which is shown in Fig 3. In this figure, recent results of balloon experiments are also shown. The experimental and modeling results are in satisfactory agreement, however we didn't take into account a solar modulation of antiproton flux and the production of third generation of antiprotons due to inelastic scattering of the antiproton flux during its confinement time in the Galaxy.

4. The Earth's antiproton radiation belt

We adopted the same approach for modeling the magnetospheric trapped antiproton flux around $L = 1.2$ in the geomagnetic equatorial region. The trapped particles at $L = 1.2$ possess a narrow pitch-angle distribution around $90°\pm20°$ and produce antiprotons will be trapped. From the criteria $R_c/R_L \leq 10$, we estimate that antiprotons that could be trapped at $L = 1.2$ have maximum kinetic energy of

$E_{crit} = 1.0$ GeV. The corresponding escape length λ_{esc} is defined as $\lambda_{esc} = \upsilon\rho\tau_{esc}$ where υ is an antiproton velocity and ρ is an atmospheric density at $L = 1.2$. The λ_{esc} is equal to infinity for particle with energy below E_{crit} and equals zero for the energies much greater than E_{crit}. In the modeling of the trapped magnetospheric antiproton flux we employed the same Eq.4 with the parameters corresponding to the atmospheric elemental composition. The results of the numerical integration of Eq.4 are shown in Fig 6. The interstellar fluxes are compared in the same figure. The magnetospheric antiproton fluxes exhibit soft spectrum which sharply falls to zero at $\sim E_{crit}$. At energies lower than 1- 2 GeV the magnetospheric trapped antiproton fluxes are about 50 - 100 times greater than the interstellar fluxes.

In this first approach, we neglect the contribution of albedo antineutrons.

5.   Conclusion

The modeling considered here for the production of antiprotons utilized nuclear interactions between cosmic ray nuclei with energies above the reaction threshold of 6 GeV and the constituents of the environment. Initially, we proceeded with the production of antiprotons in interstellar space and conferred with the balloon measurements. In the next step, we calculated the antiproton contribution due to the cosmic ray nuclei interactions with the atmospheric constituents H, He and O species at altitudes of $L = 1.2$, in the near Earth environment, to examine the viability of the formation of an antiproton belt. We obtained large fluxes compared to the interstellar fluxes by factors 50 to 100 at energies < 1 GeV. However, during strong geomagnetic storms the trapped radiation can be scattered into lower atmospheric altitudes of the same L-shells or dislocate to other L-shells which could possibly contaminate interstellar flux measurements.

1. Boezio M. et al. 1999, ApJ 518, 457
2. Boezio M. et al. 2001, Proc. 27th ICRC 5, 1695
3. Dementyev A.V., Sobolevsky N.M. 1999, Radiation Measurements 30, 553
4. Gusev A.A. et al. 2001, JGR 106, 26111
5. Jones F.C., Lukasiak A., Ptuskin V.S. 2001, ApJ 547, 264
6. Sina R., Ptuskin V.S, Seo E.S. 2001, Adv. Space Res. 27, 705
7. Spjeldvik W.N. et al. 1998, Annales Geophysicae 16, 931-939